Dynamics of locomotion in the seed harvesting ant *Messor barbarus:* Effect of individual body mass and transported load mass

Hugo Merienne [1], **Gérard Latil** [1], **Pierre Moretto** [1], **Vincent Fourcassié** [Corresp. 1]

[1] Centre de Biologie Intégrative - Centre de Recherches sur la Cognition Animale, Centre National de la Recherche Scientifique - Université de Toulouse, Toulouse, France

Corresponding Author: Vincent Fourcassié
Email address: vincent.fourcassie@univ-tlse3.fr

Ants are well-known for their amazing load carriage performances. Yet, the biomechanics of locomotion during load transport in these insects has so far been poorly investigated. Here, we present a study of the biomechanics of unloaded and loaded locomotion in the polymorphic seed-harvesting ant *Messor barbarus* (Linnaeus, 1767). This species is characterized by a strong intra-colonial size polymorphism with allometric relationships between the different body parts of the workers. In particular, big ants have much larger heads relative to their size than small ants. Their center of mass is thus shifted forward and even more so when they are carrying a load in their mandibles. We investigated the dynamics of the ant center of mass during unloaded and loaded locomotion. We found that during both unloaded and loaded locomotion, the kinetic energy and gravitational potential energy of the ant center of mass are in phase, which is in agreement with what has been described by other authors as a grounded-running gait. During unloaded locomotion, small and big ants do not display the same posture. However, they expend the same amount of mechanical energy to raise and accelerate their center of mass per unit of distance and per unit of body mass. While carrying a load, compared to the unloaded situation, ants seem to modify their locomotion gradually with increasing load mass. Therefore, loaded and unloaded locomotion do not involve discrete types of gait. Moreover, small ants carrying small loads expend less mechanical energy per unit of distance and per unit of body mass and their locomotion thus seem more mechanically efficient.

Dynamics of locomotion in the seed harvesting ant *Messor barbarus:* effect of individual body mass and transported load mass

Hugo Merienne[1], Gérard Latil[1], Pierre Moretto[1], Vincent Fourcassié[1]

[1] Centre de Recherches sur la Cognition Animale, Centre de Biologie Intégrative, Université de Toulouse, CNRS, UPS, France.

Corresponding Author:
Vincent Fourcassié

Email adress : vincent.fourcassie@univ-tlse3.fr

Street adress : Centre de Recherches sur la Cognition Animale (UMR 5169) - Centre de Biologie Intégrative - CNRS - Université Paul Sabatier - Bât 4R3. 710, cours Rosalind Franklin. 118, route de Narbonne. 31062 Toulouse cedex 09 - France

Abstract (500 words or 3000 characters)

Ants are well-known for their amazing load carriage performances. Yet, the biomechanics of locomotion during load transport in these insects has so far been poorly investigated. Here, we present a study of the biomechanics of unloaded and loaded locomotion in the polymorphic seed-harvesting ant *Messor barbarus* (Linnaeus, 1767). This species is characterized by a strong intra-colonial size polymorphism with allometric relationships between the different body parts of the workers. In particular, big ants have much larger heads relative to their size than small ants. Their center of mass is thus shifted forward and even more so when they are carrying a load in their mandibles. We investigated the dynamics of the ant center of mass during unloaded and loaded locomotion. We found that during both unloaded and loaded locomotion, the kinetic energy and gravitational potential energy of the ant center of mass are in phase, which is in agreement with what has been described by other authors as a grounded-running gait. During unloaded locomotion, small and big ants do not display the same posture. However, they expend the same amount of mechanical energy to raise and accelerate their center of mass per unit of distance and per unit of body mass. While carrying a load, compared to the unloaded situation, ants seem to modify their locomotion gradually with increasing load mass. Therefore, loaded and unloaded locomotion do not involve discrete types of gait. Moreover, small ants carrying small loads expend less mechanical energy per unit of distance and per unit of body mass and their locomotion thus seem more mechanically efficient.

Introduction

Locomotion is a crucial aspect of animal behavior. It is essential to accomplish tasks such as searching for food or a shelter, hunting for prey, looking for a mate or escaping a predator. For each of these tasks animals have to adjust specific features of their locomotion in order to behave optimally (Halsey, 2016). For example, they should minimize the distance traveled and the energy expended when searching for food whereas they should rather maximize their speed when attempting to escape a predator. Different ways of moving are thus used by animals, each most fitted to a given situation. These distinct ways of moving correspond to what is called a gait, i.e., according to the definition proposed by Alexander (1989) a "*pattern of locomotion*

characteristic of a limited range of speeds described by quantities of which one or more change discontinuously at transition to other gaits".

Two main approaches are commonly used in biomechanics to investigate locomotory gaits. The first approach, which has been used in many animals (see Kar *et al*., 2003 for a review), is based on the study of the kinematics of locomotion, especially the footfall (or stepping) pattern. It consists in measuring variables such as stride frequency, stride length, leg positioning and inter-leg coordination. It allows for instance to distinguish walking, trotting and galloping in horses (Robilliard *et al*., 2007). The second approach models the individual as its center of mass (CoM) and study its dynamics. The trajectory of the CoM of an animal during locomotion can then be recorded either by integrating the ground reaction forces of its legs (Cavagna, 1975) or by video recording its displacement and analyzing the videos (Cavagna & Kaneko, 1977; Heglund *et al.*, 1995; Fumery *et al.*, 2018). From the trajectory of the CoM one can then compute the kinetic and gravitational potential energy of the CoM and investigate their variation during a stride (Heglund *et al.*, 1995; Vereecke *et al.*, 2006; Reilly *et al.*, 2007). Using this approach, Cavagna *et al*. (1977) found that during bipedal locomotion in humans, the kinetic and gravitational potential energy of the CoM are mostly in phase during walking while they are mostly out of phase during running. This kind of approach has been used to distinguish different gaits in a variety of animals, from vertebrates (birds, kangaroo rats, chipmunk and squirrels: Heglund *et al*., 1982; lizards: Farley and Ko, 1997; frogs: Ahn *et al.,* 2004; dogs: Griffin *et al*., 2004; elephants: Genin *et al.,* 2010) to invertebrates (arachnids: Sensenig and Shultz, 2007; Escalante *et al*., 2019).

Among walking animals, insects are of particular interest for the study of locomotion due to their outstanding performances, as attested by the maximum speed some insects can reach, e.g. about 40 body length per second for the ant *Cataglyphis bombycina* (Pfeffer *et al.*, 2019) or about 35 body length per second for the cockroach *Periplaneta Americana* (Full and Tu, 1991). This probably explains why insects have been for decades a source of inspiration for the design of legged robots (Kar *et al.*, 2003; Koditschek *et al.*, 2004; Dupeyroux *et al.*, 2019). From a purely kinematic point of view, the most common gait encountered in insects is the alternating tripod gait (Delcomyn, 1981) in which the swing phase of a set of three legs called tripods (the ipsilateral front and hind leg and the contralateral mid leg) is synchronized with the contact phase of the contralateral tripod. However, this pattern can be altered by many factors. For example, it can vary with the speed (Bender *et al*., 2011; Wosnitza *et al*., 2012; Mendes *et al*.,

2013; Wahl *et al*., 2015), the behavior (exploration: Reinhardt *et al*., 2009; Reinhardt and Blickhan, 2014; wall-following: Bender *et al.,* 2011; backward locomotion: Pfeffer *et al*., 2016), the external (leg amputation: Fleming and Bateman, 2007; Gruhn *et al*., 2009; Grabowska *et al*., 2012) and internal state (effects of ageing, review in Ridgel and Ritzmann, 2005; blocking of proprioceptive feed back*:* Mendes *et al*., 2013) of the insects as well as with the characteristics of their physical environment, such as the type of substrate on which they walk (Spence *et al*. 2010), the presence of wind (Full and Koehl, 1993), the slope of the terrain (Diederich, 2006; Seidl and Wehner, 2008; Moll *et al*., 2010; Grabowska *et al*., 2012; Wöhrl *et al.,* 2017), and the presence of obstacles (Watson *et al*., 2002).

One of the perturbations that is known to affect locomotory gait in humans (Ahmad and Barbosa, 2019) and other vertebrates (review by Jagnandan and Higham, 2018) but that has so far received little attention in insects is load carriage. Load carriage occurs in insects mostly internally, for example after ingesting food or when a female insect carry eggs. However, these internal loads only induce small changes in the total mass of individuals. Much more impressive are the external loads that are carried by some insects while returning to their nest. In ants in particular, these loads can be very heavy and weigh more than ten times the body mass of individuals (Bernadou *et al*., 2016). They can shift the CoM of individuals forward and thus have a strong impact on their locomotion. The changes induced by load carriage on the locomotion of ants have so far been investigated only with a kinematic approach (Zollikofer, 1994; Moll *et al*., 2013, Merienne *et al*., 2020). Consequently, little is known on the mechanical cost of locomotion and on the exchanges of energies that occur during load carriage. In particular, one does not know to what extent locomotion with a load is mechanically more costly than without a load. Since external load carriage is observed in wasps (Polidori *et al.*, 2013), which are considered as the ant ancestors, one could hypothesize that these insects could have evolved some anatomical features or mechanisms to reduce the additional cost of carrying a load on locomotion. Here, we aim to fill this gap by investigating the impact of load carriage on the CoM dynamics in individuals of the species *Messor barbarus* (Linnaeus, 1767), a Mediterranean seed-harvester ant whose workers routinely transport items weighing up to thirteen times their own mass over dozen of meters (Bernadou *et al*., 2016). Individuals of this species show a high variation in size within colonies, with a body mass ranging from 1.5 to 40.0 mg. This variation is continuous and is characterized by a positive allometry between head size and thorax length (Heredia & Detrain,

2000; Bernadou *et al.*, 2016), which means that the head of large workers is bigger than that of small workers relative to their size. Consequently, the center of mass of big workers is shifted forward compared to that of small workers (Bernadou *et al*., 2016; see also Anderson et al., 2020 for ants of the genus *Pheidole*) and one can hypothesize that this may impact the mechanical features of both unloaded and loaded locomotion differently in ants of different sizes. Moreover, because of the allometric nature of the size polymorphism, ants of different sizes may be affected differently for loads representing the same amount of individual body mass. In our study we thus chose to investigate both the effect of body mass and load mass on the locomotion of loaded ants. We varied in a systematic way the mass of the load carried by ants of different sizes and compared the displacement of the CoM and its mechanical work, which represents the amount of energy needed to raise the CoM and accelerate it during locomotion, of the same individuals in unloaded and loaded condition.

Material and methods

Studied species

Experiments were carried out with a large colony of *M. barbarus* collected in April 2018 at St Hippolyte (Pyrénées Orientales) on the French Mediterranean coast. Workers in the colony ranged from 2 to 15 mm in length and from 1 to 40 mg in mass. The colony was housed in glass tubes with a water reservoir at one end and was kept in a room at 26°C with a 12:12 L/D regime. The tubes were placed in a box (LxWxH: 0.50x0.30x0.15 m) whose walls were coated with Fluon® to prevent ants from escaping. During the experimental period, ants were fed with a mixture of seeds of various species and had access *ad libitum* to water.

Experimental setup

Ants were tested on a setup designed and built by a private company (R&D Vision, France. http://www.rd-vision.com). It consisted in a walking platform surrounded by five high speed cameras (JAI GO-5000M-PMCL: frequency: 250Hz; resolution: 30µm/px for the top camera, 20µm/px for the others). One camera was placed above the platform and four were placed on its sides. The platform was 160mm long and 25mm wide and was covered with a piece of black paper (Canson®, 160g/m^2). Four infrared spots (λ=850nm, pulse frequency: 250 Hz)

synchronized with the cameras illuminated the scene from above. The mean temperature in the middle of the platform, measured with an infrared thermometer (MS pro, Optris, USA, http://www.optris.com) over the course of the experiment, was (mean ± SD) 28 ± 1.4 °C.

Experimental protocol

We performed all experiments between April and July 2018.

We wanted to make sure that the ants we tested were foraging workers. Therefore, the first day of an experimental session, we selected a random sample of workers returning to their nest with a seed on a foraging trail established between the box containing the colony and a seed patch. We then kept these ants in a separate box and used them in our experiments the following days.

Each ant was tested twice: the first time unloaded and the second time loaded with a fishing lead glued on its mandibles. Before being tested, unloaded ants were first weighed to the nearest 0.1 mg with a precision balance (NewClassic MS semi-micro, Mettler Toledo, United Sates). Individual ants were then gently placed at one end of the platform and we started recording their locomotion as soon as they entered the camera fields. The recording was retained only if ants walked straight for at least three full strides. All videos were subsequently cropped to a whole number of strides, a stride being defined as the interval of time elapsed between two consecutive lift off of the right mid leg. To stimulate the ants and to obtain a straighter path, an artificial pheromone trail was laid down along the middle axis of the platform by depositing every centimeter a small drop of a hexane solution of Dufour gland (1 gland / 20µl) which is responsible for the production of trail pheromone in *M. barbarus* (Heredia and Detrain, 2000). This operation was renewed every 45 minutes in order to keep a fresh trail on the platform.

Once five ants were tested in unloaded condition, we proceeded with the test in loaded condition. First, each ant was anesthetized by putting it in a vial plunged in crushed ice. It was then fixed on its back, with its head maintained horizontally, and we glued a calibrated fishing lead on its mandibles with a droplet of superglue (Loctite, http://www.loctite.fr). After letting the glue dry for 15 minutes and the ant recover for half an hour, the ant was placed again on the platform and its locomotion was recorded in loaded condition. We retained only the recordings in which the load did not touch the ground during the transport. At the end of the recording, the ant was

captured and weighed a second time. It was then killed and each of its body parts (head, thorax, gaster) was weighed separately.

Data extraction and analysis

In order to compute the 3D displacement of the ants' main body parts (head, thorax, gaster) and of its overall center of mass (CoM), we tracked several anatomic points on the top view (Fig. 1A-C) and side view (Fig. 1B-D) of the videos with the software Kinovea (version 0.8.15, https://www.kinovea.org).

Assuming a homogeneous distribution of the mass within each body parts, we computed the (X, Y) coordinates of the CoM of the three main body parts (plus the load) as the mean of the (X, Y) coordinates of the two points tracked at their extremities on the top view and the vertical position (Z) as the mean of the vertical position of the two points tracked on each of these parts on the side view. For each frame we computed the position of the overall CoM as the barycenter of the CoM of its three main body parts (plus the load for loaded ants) weighted by their mass. For each ant tested, we delimited the different strides on the videos and then, for each stride, we calculated the positions (X, Y, Z) and velocity vectors of the overall CoM over multiple stride cycles. Finally, we averaged the CoM speeds and positions across the multiple stride cycles in order to obtain a single mean trajectory of the CoM in each condition (unloaded and loaded).

In order to characterize the mean trajectories of the CoM for each ant and condition, we computed the peak-to-peak amplitude of the Z positions of the CoM and assessed the sinus-like behavior of the changes in Z positions and the norm of the velocity vectors. In order to do so, we first normalized the Z positions and the norm of the velocity vectors by their respective peak-to-peak amplitude and fitted a sinus function to the resulting signals. We then computed the root-mean-square error (RMSE) between the fitted function and the normalized data.

In order to assess the general posture of the ants during locomotion, we also computed the mean Z position of their CoM in units of body length and the mean inclination angle of their body during locomotion (defined as the angle between the horizontal X axis and the line linking the gaster and head CoMs).

From the dynamic of the CoM, we then computed its kinetic (E_k) and gravitational potential (E_p) energies relative to the surroundings with the formulae

$$E_k = 0.5 * m * v^2 \quad (1)$$

and

$$E_p = m * g * h \quad (2)$$

where *m* is the mass of the ant (plus the mass of the load if one is carried), *v* the speed of the CoM, *g* the gravitational constant and *h* the vertical position of the CoM above the walking platform. We then computed the external mechanical energy of the CoM as the sum of the kinetic and potential energies. Finally, following Bastien *et al*. (2016), we computed the external mechanical work (W_{ext}) achieved to raise and accelerate the CoM as the sum of the positive increments of the external mechanical energy. Since ants did not walk the same distance or during the same amount of time, in order to compare the mechanical work they achieved, we divided W_{ext} by the distance travelled and thus obtained a "mechanical work per unit distance" ($W_{ext,d}$). This makes sense if one considers that locomotion is a repetitive process and that we cropped our videos to a whole number of strides. We then computed the mean external power (P_{ext}) by dividing W_{ext} by the duration of locomotion. Finally, we computed the mass specific values of $W_{ext,d}$ and P_{ext} by dividing both of these metrics by the ant mass for unloaded locomotion and the ant mass plus load mass for loaded locomotion.

Following Cavagna *et al*. (1976) we then computed the energy recovered (*R*, expressed in percentage) through the pendulum-like oscillations of the CoM with the formula :

$$R = 100 * \frac{W_k + W_p - W_{ext}}{W_k + W_p} \quad (3)$$

Where W_k is the sum of the positive increments of the kinetic energy versus time curve and W_p is the sum of the positive increments of the potential energy versus time curve. *R* is an indicator of the amount of energy transferred between the potential and the kinetic energy of the CoM due to its pendulum-like behavior: the closer the value of *R* to 100%, the more consistent the locomotor pattern is with the Inverted Pendulum System (IPS) model (Cavagna *et al*., 1977) in

which the fluctuations in E_p and E_k are perfectly out of phase, i.e. all the kinetic energy of the CoM is transformed in potential energy, and vice versa, over a stride.

In order to further characterize the relationship between E_k and E_p, we computed the Pearson correlation coefficient between E_k and E_p, and, following Ahn *et al*. (2004) and Vereecke *et al*. (2006), the percentage congruity between E_k and E_p (defined as the percentage of time E_k and E_p changed in the same direction). Finally, we fitted a sinus function to both E_k and E_p. We extracted the phase of E_k and E_p from these sinus functions and computed the difference between the two phases in order to access the phase lag between E_k and E_p (a positive value of this lag indicating that E_k is late compared to E_p).

All data analysis and graphics were done with R (version 3.5.1) run under RStudio (version 1.0.136). For the unloaded condition, all variables Y were expressed as a power law function of ant mass M: $Y = a * M^b$ (Merienne *et al.*, 2020). For each variable, we give in a table the value of the coefficients a and b, as well as the value of the variables predicted by the statistical model for the mean mass of the tested ants (12.5 mg). For the loaded condition, because we tested the same ants first loaded and then unloaded, we computed the ratio of each variable between the loaded (Y_l) and unloaded (Y_u) condition and expressed it as a power law function of both ant mass (M) and load ratio (LR), defined as 1 + (load mass/ant body mass) (Bartholomew *et al*., 1988): $\frac{Y_l}{Y_u} = c * M^d * LR^e$ (Merienne *et al.*, 2020). For each variable we give in a table the coefficients c and d for ant mass, e for load ratio, as well as the value of the variable predicted by the statistical model for the mean mass of tested ants and a load ratio of one. A positive value for the coefficient of an explanatory variable means that the response variable increases when the explanatory variable increases and vice versa.

Results

In total, 52 ants whose body mass ranged from 1.5 to 33.0 mg were tested in both unloaded and loaded conditions, with load ratio ranging from 1.2 to 7.0 (Fig. 2).

Unloaded ants: influence of body mass

The analysis of the position of the CoM shows that there was no evidence of a periodic pattern on the Y axis. On the other hand, the Z position of the CoM (Fig. 3A), as well as its speed norm (Fig. 3B), followed a periodic pattern that was well approximated by a sinus function, as shown by the low value of the RMSE (Table 1, line 1 & 2). Interestingly, the amplitude of the oscillations of the CoM Z position seems to be approximately the same for small and big ants (Fig. 3A). Indeed, the relative amplitude (expressed in units of body length, Table 1, line 3) of the oscillations of the CoM Z position, as well as its mean relative position (Table 1, line 4), decreased significantly with increasing ant mass ($F_{1,52} = 75.88$, $P<0.001$ and $F_{1,52} = 105.24$, $P<0.001$, respectively). The CoM of big ants was thus relatively lower and oscillated with a relatively smaller amplitude than that of small ants. The ant body angle was independent of ant mass (Table 1, line 5).

The variations of E_k and E_p were periodic and the amplitude of E_p was much greater than that of E_k in both small (Fig. 4A) and big ants (Fig. 4B). E_k and E_p were mostly in phase, as shown by the high values of both the correlation coefficient (Table 1, line 6) and the percentage congruity (Table1, line 7). Nevertheless, E_k and E_p were more in phase for big ants than for small ants (Fig. 5A). The phase lag between the variation of potential and kinetic energies was positive (Fig. 5B) and increased with increasing ant mass (Table 1, line 8: $F_{1,52} = 11.51$, $P=0.001$). As a consequence, E_k and E_p were more out of phase for big ants compared to small ants and thus both the correlation coefficient (Table 1, line 6) and the percentage congruity (Table 1, line 7) decreased with increasing ant mass ($F_{1,52} = 5.79$, $P=0.020$ and $F_{1,52} = 4.75$, $P=0.034$, respectively).

The external mechanical work of the CoM per unit distance ($W_{ext,d}$) increased with increasing ant mass (Fig. 6A). However, there was no relationship between the mass-specific external mechanical work of the CoM per unit distance ($W_{ext,d}/m$) and ant mass (m) (Table 1, line 9). In the same way, the mean external mechanical power of the CoM (P_{ext}) increased with increasing ant mass (Fig. 6B) but there was no relationship between the mass-specific external mechanical power of the CoM (P_{ext}/m) and ant mass (Table 1, line 10).

The percentage energy recovery was very low and did not depend on ant mass (Table 1, line 11).

Loaded ants: influence of ant mass and load ratio

In the same way as in unloaded condition, no periodicity was found in the CoM Y trajectory in loaded condition. On the Z direction, independent of ant mass, the sinus-like periodicity of the Z position of the CoM (assessed by the Z position RMSE) decreased with increasing load ratio (Fig. 3C and 3E, Table 2, line2: $F_{1,52}$=3.87, P=0.010). We found no significant changes in the relative amplitude of the oscillations of the CoM Z position (Table 2, line 3) and in the mean Z position of the CoM (Table 2, line 4) between the unloaded and loaded condition, whatever the ant mass and load ratio. The speed of the CoM in loaded condition followed a periodic pattern (Fig. 3D and 3F) that was well approximated by a sinus function, whatever the values of ant mass and load ratio (Table 2, line 1). Independent of ant mass and load ratio, the ant body angle did not change between the unloaded and loaded condition (Table 2, line 5).

In the same way as in unloaded condition, E_k and E_p were mostly in phase for low load ratio in small (Fig. 4C) and big ants (Fig. 4D), but less so for high load ratio (Fig. 4E and 4F). Independent of ant mass and load ratio, the correlation coefficient between E_k and E_p did not vary significantly between the unloaded and loaded condition, (Fig. 5A, Table 2, line 6) and the phase lag only slightly decreased (Fig. 5B, Table 2, line 8). However, independent of ant mass, the percentage congruity decreased for ants carrying loads of increasing load ratio (Table 2, line 7: $F_{1,52}$ = 8.22, P<0.001).

Independent of load ratio, the mass-specific $W_{ext,d}$ increased with increasing ant mass (Table 2, line 9: $F_{2,51}$ = 12.47, P=0.024) and, independent of ant mass, it also increased with increasing load ratio ($F_{2,51}$ = 12.47, P<0.001). However, there was no effect of the load on the mass-specific P_{ext} (Table 2, line 10). Finally, there was no significant change in percentage recovery between the unloaded and loaded condition (Table 2, line 11).

Discussion

In this study, we investigated the dynamics of locomotion of unloaded and loaded individuals of the polymorphic ant *M. barbarus*. We found that during unloaded locomotion the variations of the speed of the CoM and of its vertical position are characterized by a periodic pattern with two periods corresponding to the two steps included in one stride. These variations were well described by a sinus function, although the pattern of variation of the CoM Z position was strongly affected by load transport. The kinetic and potential energies were mostly in phase

311 during unloaded locomotion, which led to very low energy recovery values. With increasing load
312 however , the variations in potential energy became much greater than the variations in kinetic
313 energy. Therefore, ants achieved mechanical work mainly to raise their CoM rather than to
314 accelerate it. The external mechanical work ants had to perform to raise and accelerate their CoM
315 over a locomotory cycle did not vary with body mass for unloaded ants and increased with load
316 ratio for ants of same body mass.

317

318 **Unloaded ants**

319 During unloaded locomotion, the mean of the absolute Z position of the CoM, as well as the
320 amplitude of its variations, did not differ between small and big ants. Therefore, relative to their
321 size, the body of small ants was higher over the ground than that of big ants and their CoM made
322 greater vertical oscillations. This difference cannot be explained by a change in body inclination
323 because this latter did not change between small and big ants. It thus seems that small ants are
324 walking in a more erect posture than big ants. This could be related to a more excited state of
325 small ants compared to big ants in response to manipulation, as also suggested by their higher
326 locomotory speed relative to their size (Merienne *et al*. 2020). Such a difference between ants of
327 different sizes in response to threat has already been found in other ant species, e.g. the leaf-
328 cutting ant *Atta capiguara* (Hughes and Goulson, 2001), and this could be related to division of
329 labor within colonies. Further experiments should be performed to answer this question.

330 The kinetic and potential energies of the CoM were mainly in phase during unloaded
331 locomotion, which led to very low energy recovery values (7-9 %). These values are similar to
332 those reported by Full and Tu (1991) in the cockroach *Periplaneta americana* and a bit below
333 those reported in the cockroach *Blaberus discoidalis* (Full and Tu, 1990) and in the ant *Formica*
334 *polyctena* (Reinhardt and Blickhan, 2014). These values are not consistent with the inverted
335 pendulum model of Cavagna *et al*. (1977). As walking ants never display aerial phases
336 (Merienne *et al*. 2020), their locomotion is thus rather better characterized as a form of *grounded*
337 *running* (*Formica polyctena* : Reinhardt and Blickhan 2014).

338 No differences were observed in the mass specific external mechanical work nor in the mass
339 specific external mechanical power between individuals of different sizes. This is in agreement
340 with the literature, which shows that the mass specific external mechanical work is constant over

a wide range of animal species ranging from 10g to 100kg in body mass (Full & Tu, 1991; Alexander, 2005). The value we found in *M. barbarus* workers (mean ± SD : 1.082 ± 0.175 $J.m^{-1}.kg^{-1}$) is very close to that reported in the literature for a wide variety of organisms, i.e. just above 1 $J.m^{-1}.kg^{-1}$.

Loaded ants

Independent of ant mass, we did not observe any changes in the mean CoM Z position and in the amplitude of the oscillations of the CoM Z positions in loaded ants. Even if the CoM mean speed decreased in loaded ants (Merienne *et al*., 2020), this decrease seems to have little impact on the sinus-like variations of the CoM speed norm (Fig. 3D and 3F). On the other hand, the pattern of variation of the CoM Z position was strongly affected by heavy loads. The locomotion was much more jerky and the variations in the CoM Z position could not be approximated by a sinus function, especially for big ants (Fig. 3E). Moreover, because of the decrease in locomotory speed due to carrying a load (Merienne *et al.*, 2020) and the amplitude of the CoM Z position which remained unchanged, the amplitude of the variation of the CoM potential energy became much greater than the amplitude of the kinetic energy (Fig. 4C-F). The mechanical energy required to raise the CoM in loaded ants is thus much greater than that required to accelerate it in the forward direction. Therefore, the variations in the CoM potential energy and in the CoM mechanical energy are nearly identical and the external mechanical work is mostly achieved for raising the CoM.

Independent of ant mass, the mass specific mechanical work increased with load ratio. This is an unexpected result as the mass specific mechanical work is independent of load ratio in humans (Bastien *et al*., 2016). It is thus mechanically more costly for ants to move one unit of mass on one unit of distance during loaded locomotion than during unloaded locomotion. Moreover, independent of load ratio, the mass specific mechanical work increased with ant mass, which means that the mechanical work big ants have to perform in order to raise one unit mass of their body on one unit of distance is greater than that of small ants.

Compared to unloaded locomotion, none of the gait parameters we studied was modified in a discrete way in loaded locomotion. We conclude that ants do not use a specific gait in order to carry a load. Rather, they adapt their locomotion to the mass of the load they transport.

In this study we focused only on the external mechanical work ants have to perform in order to raise and accelerate their CoM over a gait cycle. Therefore, we did not take into account the movement of the leg segments in the determination of both the position of the overall CoM and the internal mechanical work that ants have to perform in order to accelerate their legs relative to their CoM. Kram *et al*. (1997) found in the cockroach *Blaberus discoidalis* that this internal work represents about 13% of the external mechanical work generated to lift and accelerate the CoM. Considering that the stride frequency of *M. barbarus* (mean ± SD: 4.8 ± 0.9 Hz, Merienne *et al*., 2020) is lower than that of *B. discoidalis* (mean ± SD: 6.8 ± 0.8 Hz, Kram *et al*., 1997) and that the mass of the legs of the workers represents the same percentage of total body mass (10-12% for *M. barbarus*, unpublished data; 13% for *B. discoidalis*, Kram *et al*. 1997), we would expect the internal mechanical work to represent a smaller part of the total mechanical work in *M. barbarus* compared to *B. discoidalis*. Despite the technical difficulties of tracking the 3D displacement of insect legs (but see: Uhlmann *et al*. 2017), this aspect could constitute an interesting perspective for further studies.

Conclusion

Unloaded ants adopted different postures according to their size. Small ants were more erected on their legs than big ants and their CoM showed greater vertical oscillations. However, this did not affect the amount of energy per unit of distance and unit of body mass required to raise and accelerate the CoM. Both for unloaded and loaded locomotion, the kinetic and potential energies were mainly in phase, which corresponds to the grounded-running gait described by Reinhardt and Blickhan (2014) during unloaded locomotion in the ant *Formica polyctena*. Regarding loaded locomotion, the amount of energy needed to raise and accelerate the center of mass per unit of distance and unit of body mass increased with increasing body mass and load mass, suggesting that, in this respect, smaller ants carrying smaller loads were mechanically more efficient during locomotion. This could be related to the division of labor observed on the foraging trails of *M. barbarus*. In fact, relative to the proportion they represent on foraging trails, workers of intermediate size, i.e. *media*, contribute the largest share of seed transport, compared to small or big workers. Big workers are mostly present at the end of the trails where they climb on the plants to cut thick stalks or spikelets, or inside the nest, to mill the seeds and prepare them for consumption.

Acknowledgements

The authors wish to thank Ewen Powie and Loreen Rupprecht for their help in video analysis and data extraction. Thanks are also due to Melanie Debelgarric for designing the Dufour gland extraction protocol.

References

Ahmad HN, Barbosa TM. 2019. The effects of backpack carriage on gait kinematics and kinetics of schoolchildren. *Scientific Reports* 9:1–6.

Ahn AN, Furrow E, Biewener AA. 2004. Walking and running in the red-legged running frog, *Kassina maculata*. *Journal of Experimental Biology* 207:399–410.

Alexander RM. 1989. Optimization and gaits in the locomotion of vertebrates. *Physiological Reviews* 69:1199–1227.

Alexander RM. 2005. Models and the scaling of energy costs for locomotion. *Journal of experimental biology* 208:1645–1652.

Anderson, P.S.L., Rivera, M.D., Suarez, A.W. (2020). "Simple" biomechanical model for ants reveals how correlated evolution among body segments minimizes variation in center of mass as heads get larger. *Integrative and Comparative Biology,* 1–15. doi:10.1093/icb/icaa027

Bartholomew GA, Lighton JRB, Feener DH Jr. 1988. Energetics of trail running, load carriage, and emigration in the column-raiding army ant *Eciton hamatum. Physiological Zoology*, 61: 57-68.

Bastien GJ, Willems PA, Schepens B, Heglund NC. 2016. The mechanics of head-supported load carriage by Nepalese porters. *Journal of Experimental Biology* 219:3626–3634.

Bender JA, Simpson EM, Tietz BR, Daltorio KA, Quinn RD, Ritzmann RE. 2011. Kinematic and behavioral evidence for a distinction between trotting and ambling gaits in the cockroach *Blaberus discoidalis*. *Journal of Experimental Biology* 214:2057–2064.

Bernadou A, Felden A, Moreau M, Moretto P, Fourcassié V. 2016. Ergonomics of load transport in the seed harvesting ant *Messor barbarus* : morphology influences transportation method and efficiency. *Journal of Experimental Biology* 219:2920–2927.

Cavagna GA. 1975. Force platforms as ergometers. *Journal of Applied Physiology* 39:174–179.

Cavagna GA, Heglund NC, Taylor CR. 1977. Mechanical work basic mechanisms in terrestrial locomotion : two for minimizing energy expenditure. *American Journal of Physiology* 233:243–261.

436 Cavagna GA, Kaneko M. 1977. Mechanical work and efficiency in level walking and running.
437 *Journal of Physiology* 268:467–481.

438 Cavagna GA, Thys H, Zamboni A. 1976. The source of external work in level walking and
439 running. *Journal of Physiology* 262:639–657.

440 Delcomyn F. 1981. *Locomotion and Energetics in Arthropods*. Springer US.

441 Diederich B. 2006. Stick insects walking along inclined surfaces. *Integrative and Comparative*
442 *Biology* 42:165–173.

443 Dupeyroux J, Serres JR, Viollet S. 2019. AntBot: A six-legged walking robot able to home like
444 desert ants in outdoor environments. *Science Robotics* 4:1–13.

445 Escalante I, Badger MA, Elias DO. 2019. Variation in movement : multiple locomotor gaits in
446 Neotropical harvestmen. *Biological Journal of the Linnean Society* 20:1–15.

447 Farley CT, Ko TC. 1997. Mechanics of locomotion in lizards. *Journal of Experimental Biology*
448 200:2177–2188.

449 Fleming PA, Bateman PW. 2007. Just drop it and run: the effect of limb autotomy on running
450 distance and locomotion energetics of field crickets (*Gryllus bimaculatus*). *Journal of*
451 *Experimental Biology* 210:1446–1454.

452 Full RJ, Koehl MR. 1993. Drag and lift on running insects. *Journal of Experimental Biology*
453 176:89–101.

454 Full RJ, Tu MS. 1990. Mechanics of six-legged runners. *Journal of experimental biology*
455 148:129–146.

456 Full RJ, Tu MS. 1991. Mechanics of a rapid running insect: two-, four- and six-legged
457 locomotion. *Journal of Experimental Biology* 231:215–231.

458 Fumery, G., Claverie, L., Fourcassié, V., Moretto, P. 2018. Walking pattern efficiency during
459 collective load transport. *Gait & Posture*, 64: 244-247. doi:10.1016/j.gaitpost.2018.06.114

460 Genin JJ, Willems PA, Cavagna GA, Lair R, Heglund NC. 2010. Biomechanics of locomotion in
461 Asian elephants. *Journal of Experimental Biology* 213:694–706.

462 Grabowska M, Godlewska E, Schmidt J, Daun-Gruhn S. 2012. Quadrupedal gaits in hexapod

463 animals - inter-leg coordination in free-walking adult stick insects. *Journal of Experimental*
464 *Biology* 215:4255–4266.

465 Griffin TM, Main RP, Farley CT. 2004. Biomechanics of quadrupedal walking: how do four-
466 legged animals achieve inverted pendulum-like movements? *Journal of experimental*
467 *biology* 207:3545–3558.

468 Gruhn M, Zehl L, Büschges A. 2009. Straight walking and turning on a slippery surface. *Journal*
469 *of Experimental Biology*, 212: 194-209.

470 Halsey LG. 2016. Terrestrial movement energetics: current knowledge and its application to the
471 optimising animal. *Journal of Experimental Biology* 219:1424–1431.

472 Heglund NC, Cavagna GA, Taylor CR. 1982. Energetics and mechanics of terrestrial
473 locomotion. III. Energy changes of the centre of mass as a function of speed and body size
474 in birds and mammals. *Journal of Experimental Biology* 97:41–56.

475 Heglund NC, Willems PA, Penta M, Cavagna GA. 1995. Energy-saving gait mechanics with
476 head-supported loads. *Letters to Nature* 375:52–53.

477 Heredia A, Detrain C. 2000. Worker size polymorphism and ethological role of sting associated
478 glands in the harvester ant *Messor barbarus*. *Insectes Sociaux* 47:383–389.

479 Hughes WOH, Goulson D. 2001. Polyethism and the importance of context in the alarm reaction
480 of the grass-cutting ant, *Atta capiguara*. *Behavioral Ecology and Sociobiology* 49:503–508.

481 Jagnandan K, Higham TE. 2018. How rapid changes in body mass affect the locomotion of
482 terrestrial vertebrates: Ecology, evolution and biomechanics of a natural perturbation.
483 *Biological Journal of the Linnean Society* 124:279–293.

484 Kar DC, Kurien Issac K, Jayarajan K. 2003. Gaits and energetics in terrestrial legged
485 locomotion. *Mechanism and Machine Theory* 38:355–366.

486 Koditschek DE, Full RJ, Buehler M. 2004. Mechanical aspects of legged locomotion control.
487 *Arthropod Structure and Development* 33:251–272.

488 Kram R, Wong B, Full RJ. 1997. Three-dimensional kinematics and limb kinetic energy of
489 running cockroaches. *Journal of Experimental Biology* 200:1919–29.

490 Mendes CS, Bartos I, Akay T, Márka S, Mann RS. 2013. Quantification of gait parameters in

freely walking wild type and sensory deprived *Drosophila melanogaster*. *eLife* 2013:1–24.

Merienne H, Latil G, Moretto P, Fourcassié V 2020. Walking kinematics in the polymorphic seed harvester ant *Messor barbarus:* influence of body size and load carriage. *Journal of Experimental Biology,* 223: jeb205690 doi: 10.1242/jeb.205690

Moll K, Roces F, Federle W. 2010. Foraging grass-cutting ants (*Atta vollenweideri*) maintain stability by balancing their loads with controlled head movements. *Journal of Comparative Physiology* 196:471–480.

Moll K, Roces F, Federle W. 2013. How load-carrying ants avoid falling over: mechanical stability during foraging in *Atta vollenweideri* grass-cutting ants. *PLoS ONE* 8:1–9.

Pfeffer, S.E., Wahl, V.L., Wittlinger, M., Wolf, H. 2019. High-speed locomotion in the Saharan silver ant, Cataglyphis bombycina. *Journal of Experimental Biology*, 222, jeb198705. doi:10.1242/jeb.198705

Pfeffer SE, Wahl VL, Wittlinger M. 2016. How to find home backwards? Locomotion and inter-leg coordination during rearward walking of *Cataglyphis fortis* desert ants. *Journal of Experimental Biology* 219:2110–2118.

Polidori, C., Crottini, A., Venezia, D., Selfa, J., Saino, N., Rubolini, D. 2013. Food load manipulation ability shapes flight morphology in females of central-place foraging Hymenoptera. *Frontiers in Zoology*, 10. doi:10.1186/1742-9994-10-36

Reilly SM, McElroy EJ, Biknevicius AR. 2007. Posture, gait and the ecological relevance of locomotor costs and energy-saving mechanisms in tetrapods. *Zoology* 110:271–289.

Reinhardt L, Blickhan R. 2014. Level locomotion in wood ants: evidence for grounded running. *Journal of Experimental Biology* 217:2358–2370.

Reinhardt L, Weihmann T, Blickhan R. 2009. Dynamics and kinematics of ant locomotion: do wood ants climb on level surfaces? *Journal of Experimental Biology* 212:2426–2435.

Ridgel AL, Ritzmann RE. 2005. Insights into age-related locomotor declines from studies of insects. *Ageing Research Reviews* 4:23–39.

Robilliard JJ, Pfau T, Wilson AM. 2007. Gait characterisation and classification in horses. *Journal of Experimental Biology* 210:187–197.

519 Seidl T, Wehner R. 2008. Walking on inclines: how do desert ants monitor slope and step length.
520 *Frontiers in Zoology* 5:1–15.

521 Sensenig AT, Shultz JW. 2007. Mechanical energy oscillations during locomotion in the
522 harvestman *Leiobunum vittatum* (Opiliones). *Journal of Arachnology* 34:627–633.

523 Spence AJ, Revzen S, Seipel J, Mullens C, Full RJ. 2010. Insects running on elastic surfaces.
524 *Journal of Experimental Biology* 213:1907–1920.

525 Uhlmann V, Ramdya P, Delgado-Gonzalo R, Benton R, Unser M. 2017. FlyLimbTracker: An
526 active contour based approach for leg segment tracking in unmarked, freely behaving
527 Drosophila. *PLoS ONE* 12:1–21.

528 Vereecke EE, D'Août K, Aerts P. 2006. The dynamics of hylobatid bipedalism: evidence for an
529 energy-saving mechanism? *Journal of Experimental Biology* 209:2829–2838.

530 Wahl V, ·Pfeffer SE, Wittlinger M. 2015. Walking and running in the desert ant *Cataglyphis*
531 *fortis*. Journal of comparative Physiology A, 201: 645-656.

532 Watson JT, Ritzmann RE, Zill SN, Pollack AJ. 2002. Control of obstacle climbing in the
533 cockroach, *Blaberus discoidalis*. I. Kinematics. *Journal of Comparative Physiology A:*
534 *Neuroethology, Sensory, Neural, and Behavioral Physiology* 188:39–53.

535 Wöhrl T, Reinhardt L, Blickhan R. 2017. Propulsion in hexapod locomotion: how do desert ants
536 traverse slopes? *Journal of Experimental Biology* 220:1618–1625.

537 Wosnitza a., Bockemuhl T, Dubbert M, Scholz H, Buschges A. 2012. Inter-leg coordination in
538 the control of walking speed in Drosophila. *Journal of Experimental Biology* 216:480–491.

539 Zolliköfer CPE. 1994. Stepping patterns in ants - Part III - Influence of load. *The Journal of*
540 *Experimental Biology* 192:119–127.

541

542

Table 1: ***Influence of body mass on the kinematics of unloaded ants.*** *Each line gives the results of a power law model describing the influence of ant mass M (in mg) on each variables studied Y, following the equation $Y=a*M^b$. The first column corresponds to the model prediction and 95% confidence interval for the mean value of ant mass (12.5 mg). The second column gives the value of the coefficient a and its 95% confidence interval, the third column the value of the coefficient b for ant mass and its 95% confidence interval, and the fourth column the adjusted R^2 for the model. BL= body length. Bold characters indicate that 0 is not included in the 95% confidence interval of the coefficient b for ant mass. N = 52 ants.*

Table 2: ***Influence of body mass and load ratio on the changes in kinematics between unloaded and loaded locomotion.*** *Each line gives the result of a power law model describing the influence of ant mass M (in mg) and load ratio LR on the relative changes of variables Y between the loaded and unloaded condition. The corresponding equation is $Y_l/Y_u = c * M^d * LR^e$ where Y_u corresponds to the value of the variable in the unloaded condition and Y_l to the value of the same variable in the loaded condition. The first column corresponds to the model prediction and 95% confidence interval for the mean value of ant mass (12.5 mg) and a load ratio of 1 (unloaded ants). The second column gives the value of the coefficient c and its 95% confidence interval, the third column the value of the coefficient d for ant mass and its 95% confidence interval, the fourth column the value of the coefficient e for the load ratio and its 95% confidence interval and the fifth column the adjusted R^2 for the model. A positive value for a coefficient (i.e. c, d or e) means that the value of the response variable in loaded condition increases compared to unloaded condition when the explanatory variable increases and vice versa. BL= body length. Bold characters indicate that 0 is not included in the 95% confidence interval of the coefficient d for ant mass and e for load ratio. Because the path followed by ants was straight, the values of the variables for the right and left leg of each pair of legs were averaged. N = 52 ants.*

543

Figure 1: ***Location of the points tracked on each ant.*** *The snapshots show a top view (A, C) and a side view (B, D) of the same ant (ant mass = 10.1 mg) tested in unloaded (A, B) and loaded condition (C, D) (load mass = 3.5mg). In C) the X axis corresponds to the longitudinal body axis while the Y axis corresponds to the transverse body axis. The position of the tracked points is represented in red.*

Figure 2: ***Body mass and load ratio of tested ants.*** *The points represent small ants (blue, N = 27), big ants (red, N = 27), low load ratio (empty dots, N = 27) and high load ratio (filled dots, N = 27).*

Figure 3: ***Variations of the vertical position and norm of the velocity vector of the ant CoM.*** *The mean variation of the vertical position (**A, C, E**) and norm of the velocity vector (**B, D, F**) of the CoM are shown for **A- B**: small (**blue**, ant mass < 10.2 mg, N = 27) and big (**red**, ant mass > 10.2 m g, N = 27) unloaded ants over one stride cycle. **C-D**: small (**blue**, ant mass < 10.2 mg, N = 9) and big (**red**, ant mass > 10.2 mg, N = 18) ants loaded with small load ratio (LR<3). **E-F**: small (**blue**, ant mass < 10.2 mg, LR > 3, N = 17) and big (**red**, ant mass > 10.2 mg, LR > 3, N = 10) ants loaded with high load ratio (LR>3). The dashed lines represent the 95% confidence interval of the mean. For the sake of clarity, all values are centered on their mean.*

Figure 4: ***Variations of the mechanical energies of the CoM relative to the surroundings.*** *The mean variation of the kinetic (**orange**), potential (**light blue**) and external mechanical (**black**) energies over one stride cycle are shown for **A**: small unloaded ants (ant mass < 10.2 mg, N = 27); **B**: big unloaded ants (ant mass > 10.2 mg, N = 27); **C**: small loaded ants with small load ratio (ant mass < 10.2 mg, load ratio < 3, N = 9); **D**: big loaded ants with small load ratio (ant mass > 10.2 mg, load ratio < 3, N = 17); **E**: small loaded ants with high load ratio (ant mass < 10.2 mg, load ratio > 3, N = 18); **F**: big loaded ants with high load ratio (ant mass > 10.2 mg, load ratio > 3, N = 10). For the sake of clarity, the values of energies are centered on their mean.*

Figure 5: ***Correlation coefficient and phase lag between the kinetic and potential energies of the CoM.*** *Correlation coefficient (**A**) and phase lag (**B**) between the CoM E_p and E_k for unladen ants and loaded ants. The results are shown for small (blue) and big ants (red). Different letters above the bars indicate that the differences between samples is significant according to a Welch two sample t-test (P<0.05). The line within the box represents the median, the lower and upper boundaries represent respectively the 25^{th} and 75^{th} percentiles while the whiskers extend to the smallest and largest values within 1.5 box lengths. The notch in each bar represents the confidence interval of the median. N= 52 ants.*

*Figure 6****: External mechanical work and power for unloaded ants.*** ***A****: external mechanical work ($F_{1,52}$ =1502, P<0.001) and **B**: external mechanical power ($F_{1,52}$ =717, P<0.001). The straight line gives the prediction of a linear regression model and the dashed lines the 95% confidence interval of the slope of the regression line (N= 52 ants).*

Table 1(on next page)

Influence of body mass on the kinematics of unloaded ants.

Each line gives the results of a power law model describing the influence of ant mass M (in mg) on each variables studied Y, following the equation $Y=a*M^b$. The first column corresponds to the model prediction and 95% confidence interval for the mean value of ant mass (12.5 mg). The second column gives the value of the coefficient a and its 95% confidence interval, the third column the value of the coefficient b for ant mass and its 95% confidence interval, and the fourth column the adjusted R^2 for the model. BL= body length. Bold characters indicate that 0 is not included in the 95% confidence interval of the coefficient b for ant mass. N = 54 ants

	Variable	Model prediction for mean(ant mass) [CI]	Coefficient a [CI]	Coefficient b for ant mass [CI]	Adj R^2
1	RMSE speed norm	0.134 [0.124;0.145]	0.148 [0.119;0.184]	-0.038 [-0.129; 0.052]	0.00
2	RMSE Z position	0.143 [0.129;0.158]	0.160 [0.121;0.212]	-0.044 [-0.161; 0.073]	0.00
3	Z position amplitude (BL[1])	0.015 [0.014;0.017]	0.048 [0.037;0.062]	**-0.451 [-0.555;-0.347]**	0.59
4	Mean Z position (BL)	0.121 [0.115;0.128]	0.278 [0.238;0.324]	**-0.326 [-0.389;-0.262]**	0.67
5	Body angle (°)	11.77 [10.85;12.76]	14.71 [11.68;18.52]	-0.088 [-0.183; 0.008]	0.04
6	Correlation coefficient	0.411 [0.355;0.475]	0.695 [0.459;1.053]	**-0.206 [-0.379;-0.034]**	0.09
7	Percentage congruity (%)	66.18 [64.33;68.09]	72.62 [66.97;78.74]	**-0.036 [-0.070;-0.003]**	0.07
8	Ek / Ep phase (°)	26.42 [21.81;32.00]	9.864 [5.637;17.26]	**0.387 [0.157; 0.616]**	0.18
9	Mass specific Wext (nJ/mm/mg)	1.072 [1.027;1.120]	1.050 [0.929;1.187]	0.008 [-0.043; 0.059]	0.00
10	Mass specific Pext (nJ/s/mg)	30.94 [28.58;33.49]	29.32 [23.40;36.75]	0.021 [-0.073; 0.115]	0.00
11	Percentage recovery (%)	8.200 [7.392;9.097]	6.407 [4.770;8.606]	0.097 [-0.026; 0.219]	0.03

1 [1] BL= Body Length

Table 2(on next page)

Influence of body mass and load ratio on the changes in kinematics between unloaded and loaded locomotion

Each line gives the result of a power law model describing the influence of ant mass (in mg) and load ratio on the relative changes of variables between the loaded and unloaded condition. The corresponding equation is where corresponds to the value of the variable in the unloaded condition and to the value of the same variable in the loaded condition. The first column corresponds to the model prediction and 95% confidence interval for the mean value of ant mass (12.5 mg) and a load ratio of 1 (unloaded ants). The second column gives the value of the coefficient c and its 95% confidence interval, the third column the value of the coefficient d for ant mass and its 95% confidence interval, the fourth column the value of the coefficient e for the load ratio and its 95% confidence interval and the fifth column the adjusted R^2 for the model. A positive value for a coefficient (i.e. c, d or e) means that the value of the response variable in loaded condition increases compared to unloaded condition when the explanatory variable increases and vice versa. BL= body length. Bold characters indicate that 0 is not included in the 95% confidence interval of the coefficient d for ant mass and e for load ratio. Because the path followed by ants was straight, the values of the variables for the right and left leg of each pair of legs were averaged. N = 54 ants.

	Variable (ratio loaded / unloaded)	Model prediction for mean(ant mass) and LR=1 [CI]	Coefficient c [CI]	Coefficient for d for ant mass [CI]	Coefficient for e for load ratio [CI]	Adj R^2
1	RMSE Speed norm	0.912 [0.679;1.225]	0.700 [0.413;1.187]	0.104 [-0.033; 0.241]	0.208 [-0.062; 0.478]	0.02
2	RMSE Z position	0.863 [0.615;1.212]	0.584 [0.318;1.072]	0.154 [-0.004; 0.311]	**0.412 [0.101; 0.722]**	0.10
3	Z position amplitude (BL[1])	1.242 [0.836;1.845]	1.115 [0.548;2.266]	0.042 [-0.141; 0.226]	0.011 [-0.352; 0.373]	0.02
4	Mean Z position (BL)	0.917 [0.755;1.113]	0.874 [0.617;1.238]	0.019 [-0.071; 0.109]	-0.062 [-0.240; 0.116]	0.01
5	Body angle (°)	0.884 [0.440;1.774]	0.645 [0.175;2.378]	0.120 [-0.226; 0.467]	-0.622 [-1.274; 0.030]	0.09
6	Correlation coefficient	1.353 [0.835;2.194]	0.996 [0.419;2.366]	0.121 [-0.104; 0.345]	-0.212 [-0.654; 0.230]	0.04
7	Percentage congruity (%)	1.116 [1.012;1.231]	1.186 [0.995;1.414]	-0.024 [-0.069; 0.022]	**-0.176 [-0.266;-0.086]**	0.22
8	Ek / Ep phase (°)	2.174 [0.766;6.171]	12.07 [1.816;80.30]	**-0.663 [-1.183;-0.143]**	**-0.995 [-1.988;-0.001]**	0.14
9	Mass specific Wext (nJ/mm/mg)	1.120 [0.917;1.367]	0.852 [0.596;1.218]	**0.107 [0.015; 0.200]**	**0.454 [0.271; 0.636]**	0.31
10	Mas specific Pext (nJ/s/mg)	1.202 [0.862;1.676]	1.153 [0.636;2.091]	0.016 [-0.138; 0.171]	-0.255 [-0.559;0.049]	0.04
11	Percentage recovery (%)	0.883 [0.571;1.367]	1.090 [0.498;2.384]	-0.082 [-0.285;0.120]	-0.144 [-0.544;0.255]	0.01

[1] BL= Body Length

Figure 1

Location of the points tracked on each ant

The snapshots show a top view (A, C) and a side view (B, D) of the same ant (ant mass = 10.1 mg) tested in unloaded (A, B) and loaded condition (C, D) (load mass = 3.5mg). In C) the X axis corresponds to the longitudinal body axis while the Y axis corresponds to the transverse body axis. The position of the tracked points is represented in red.

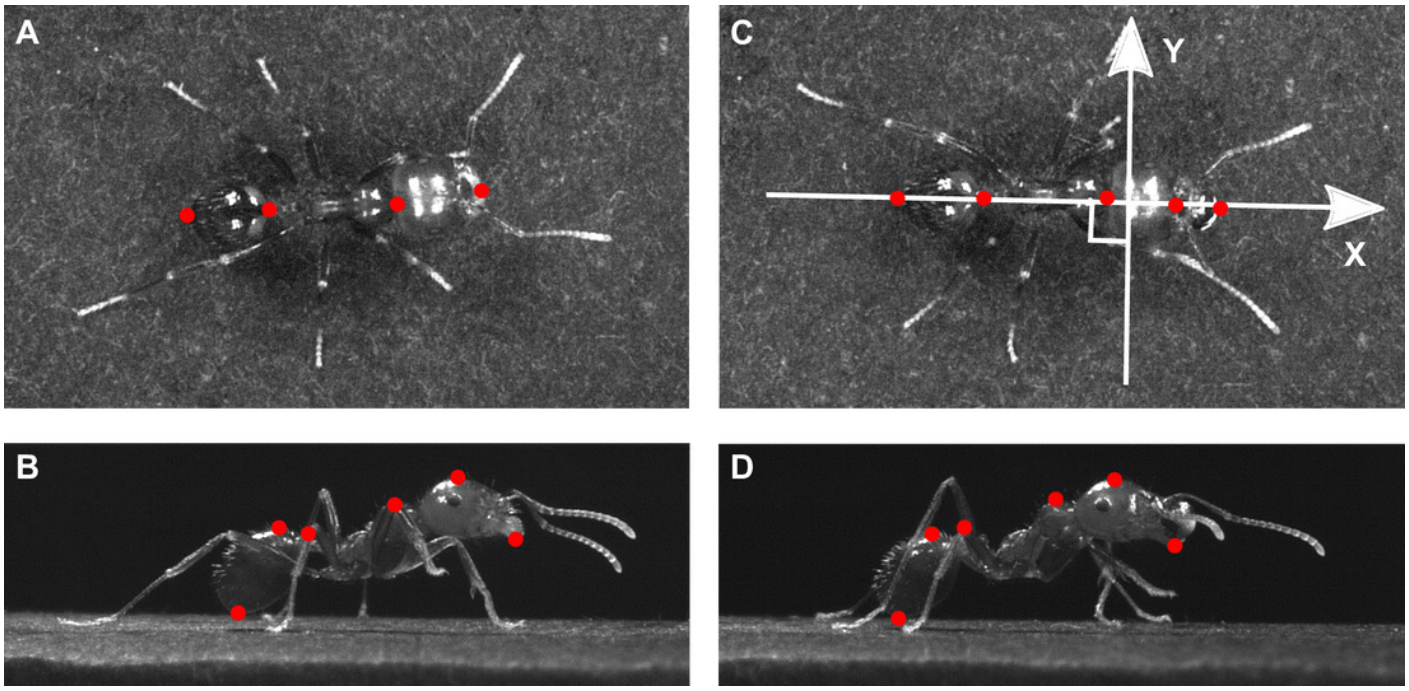

Figure 2

Body mass and load ratio of tested ants

The points represent small ants (blue, N = 27), big ants (red, N = 27), low load ratio (empty dots, N = 27) and high load ratio (filled dots, N = 27).

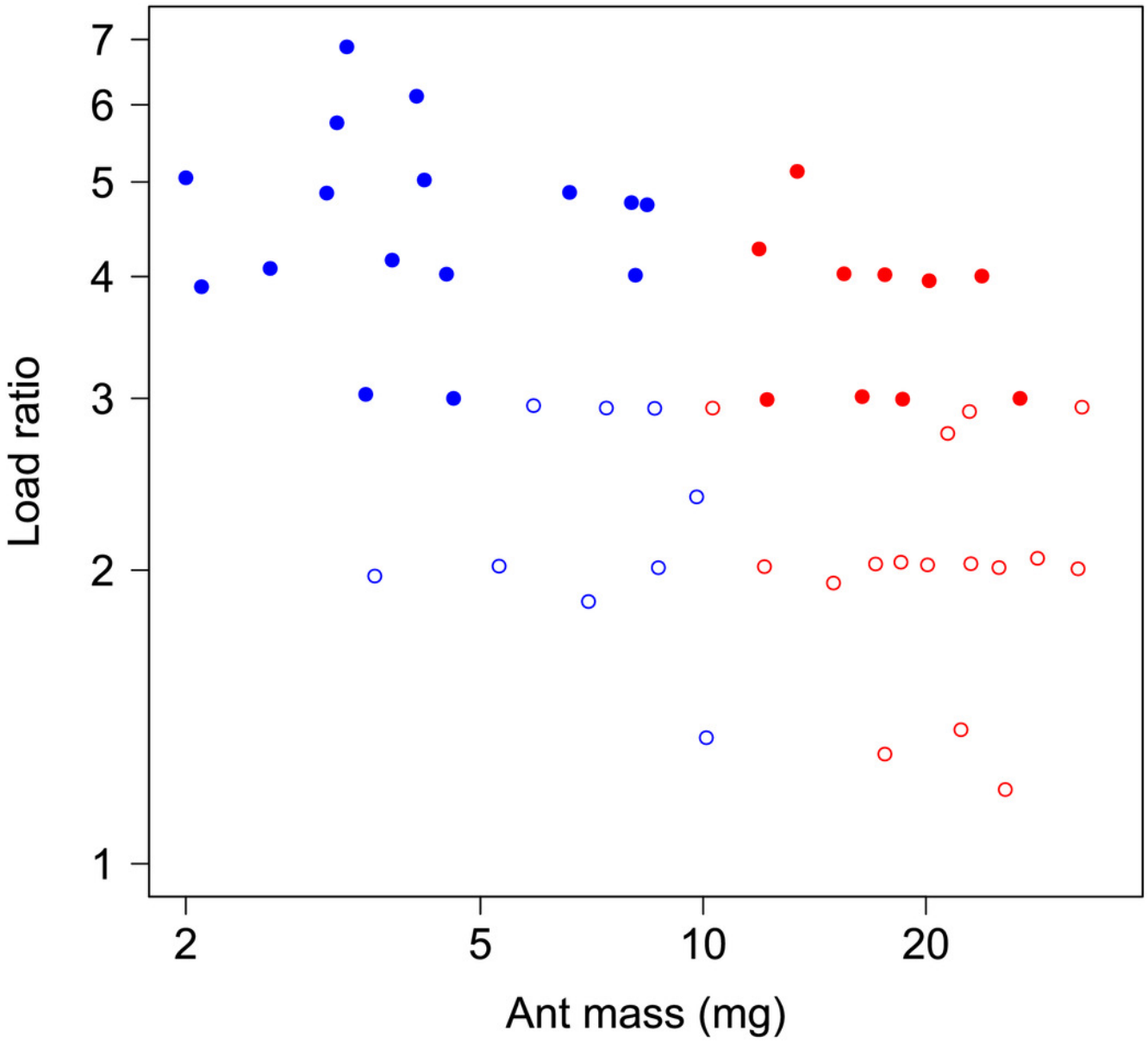
Load ratio
7
6
5
4
3
2
1
2
5
10
20
Ant mass (mg)

Figure 3

Variations of the vertical position and norm of the velocity vector of the ant CoM.

The mean variation of the vertical position (**A, C, E**) and norm of the velocity vector (**B, D, F**) of the CoM are shown for **A- B**: small (**blue**, ant mass < 10.2 mg, N = 27) and big (**red**, ant mass > 10.2 m g, N = 27) unloaded ants over one stride cycle. **C-D**: small (**blue**, ant mass < 10.2 mg, N = 9) and big (**red**, ant mass > 10.2 mg, N = 18) ants loaded with small load ratio (LR<3). **E-F**: small (**blue**, ant mass < 10.2 mg, LR > 3, N = 17) and big (**red**, ant mass > 10.2 mg, LR > 3, N = 10) ants loaded with high load ratio (LR>3). The dashed lines represent the 95% confidence interval of the mean. For the sake of clarity, all values are centered on their mean.

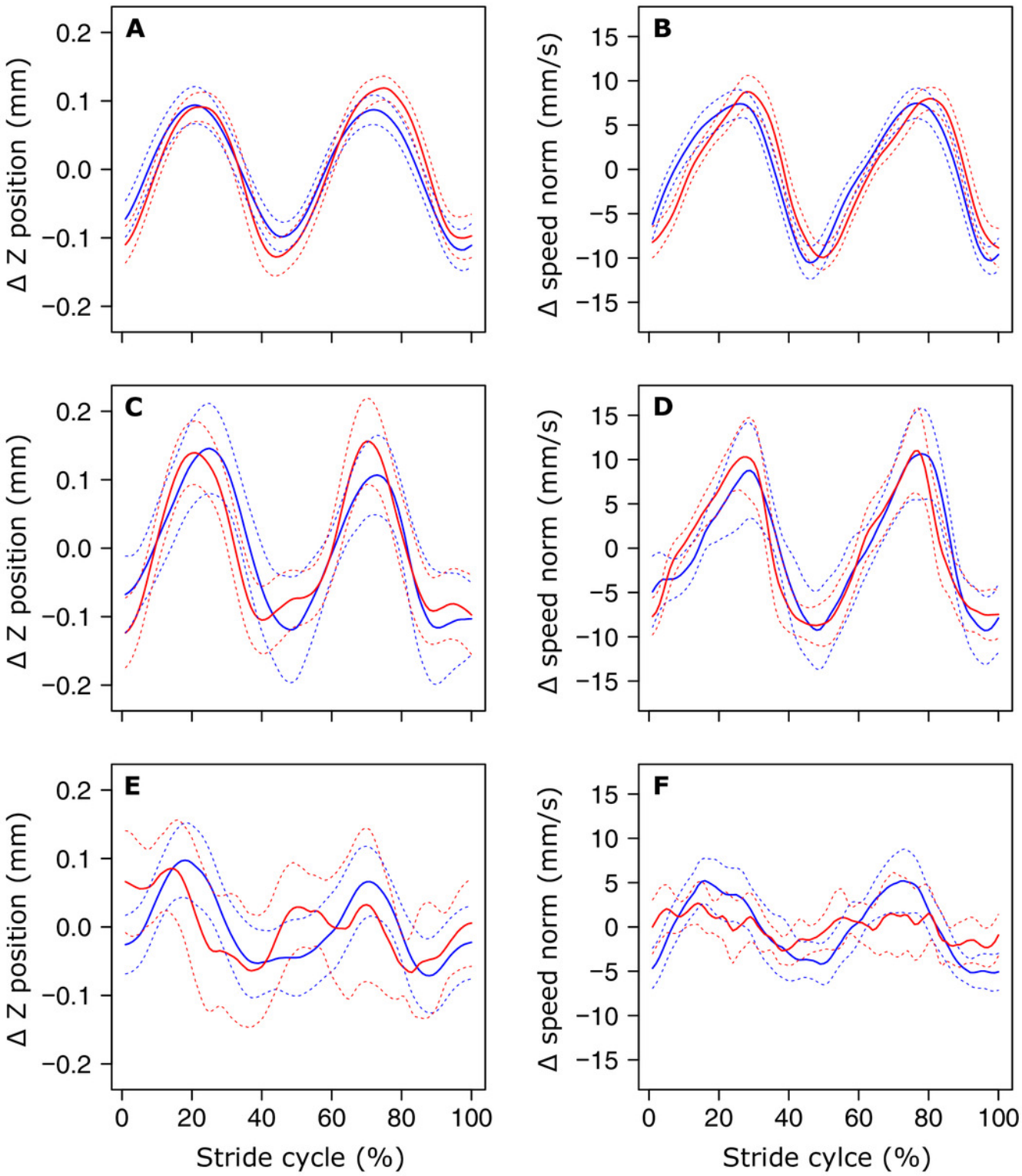
A
B
C
D
E
F
Δ Z position (mm)
Δ speed norm (mm/s)
0.2
0.1
0.0
−0.1
−0.2
15
10
5
0
−5
−10
−15
0
20
40
60
80
100
Stride cycle (%)
Stride cylce (%)

Figure 4

Variations of the mechanical energies of the CoM relative to the surroundings

The mean variation of the kinetic (**orange**), potential (**light blue**) and external mechanical (**black**) energies over one stride cycle are shown for **A**: small unloaded ants (ant mass < 10.2 mg, N = 27); **B**: big unloaded ants (ant mass > 10.2 mg, N = 27); **C**: small loaded ants with small load ratio (ant mass < 10.2 mg, load ratio < 3, N = 9); **D**: big loaded ants with small load ratio (ant mass > 10.2 mg, load ratio < 3, N = 17); **E**: small loaded ants with high load ratio (ant mass < 10.2 mg, load ratio > 3, N = 18); **F**: big loaded ants with high load ratio (ant mass > 10.2 mg, load ratio > 3, N = 10). For the sake of clarity, the values of energies are centered on their mean.

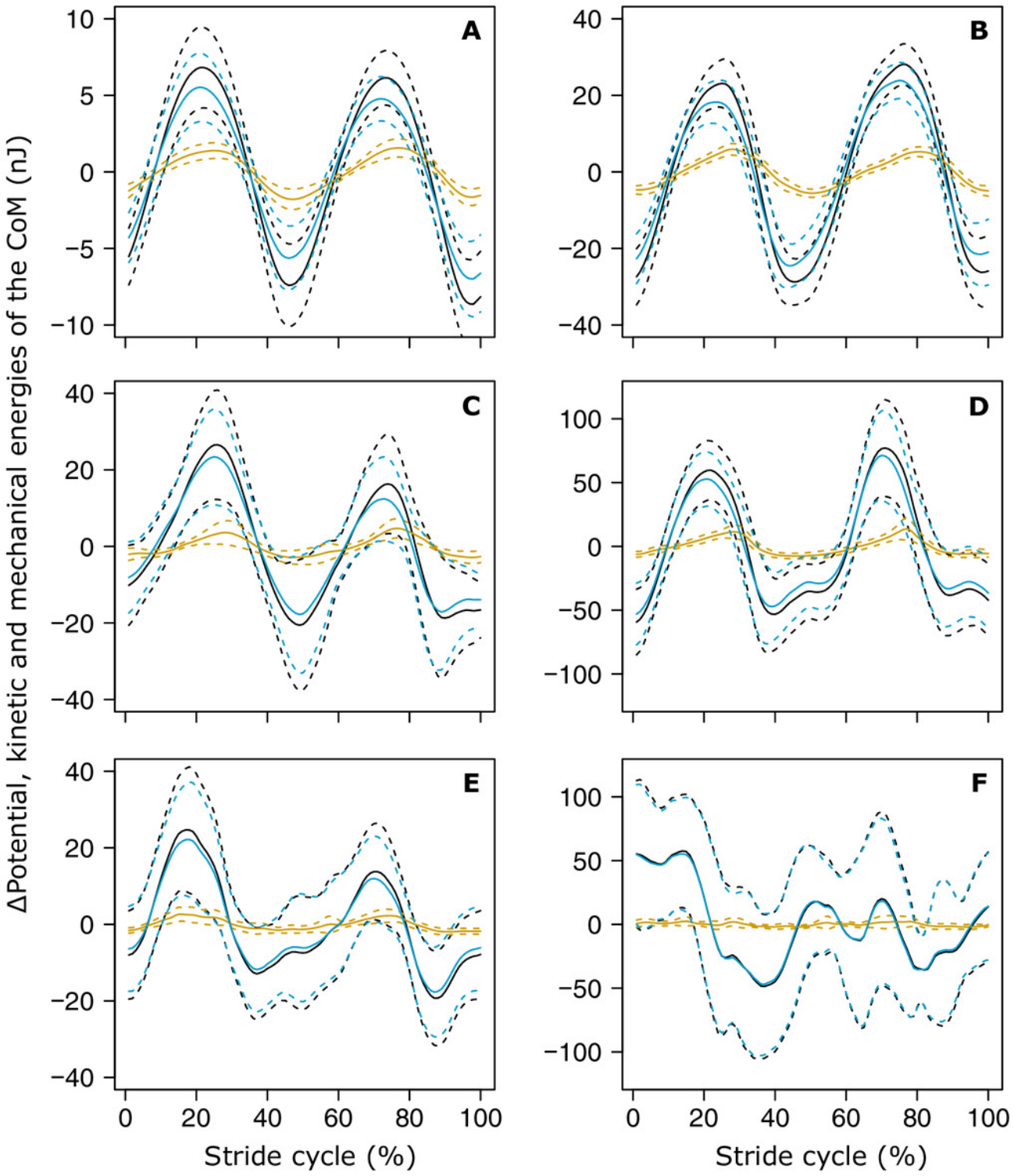
A
B
C
D
E
F
ΔPotential, kinetic and mechanical energies of the CoM (nJ)
Stride cycle (%)
Stride cycle (%)

Figure 5

Correlation coefficient and phase lag between the kinetic and potential energies of the CoM.

Correlation coefficient (**A**) and phase lag (**B**) between the CoM E_p and E_k for unladen ants and loaded ants. The results are shown for small (blue) and big ants (red). Different letters above the bars indicate that the differences between samples is significant according to a Welch two sample t-test ($P<0.05$). The line within the box represents the median, the lower and upper boundaries represent respectively the 25th and 75th percentiles while the whiskers extend to the smallest and largest values within 1.5 box lengths. The notch in each bar represents the confidence interval of the median. N= 54 ants.

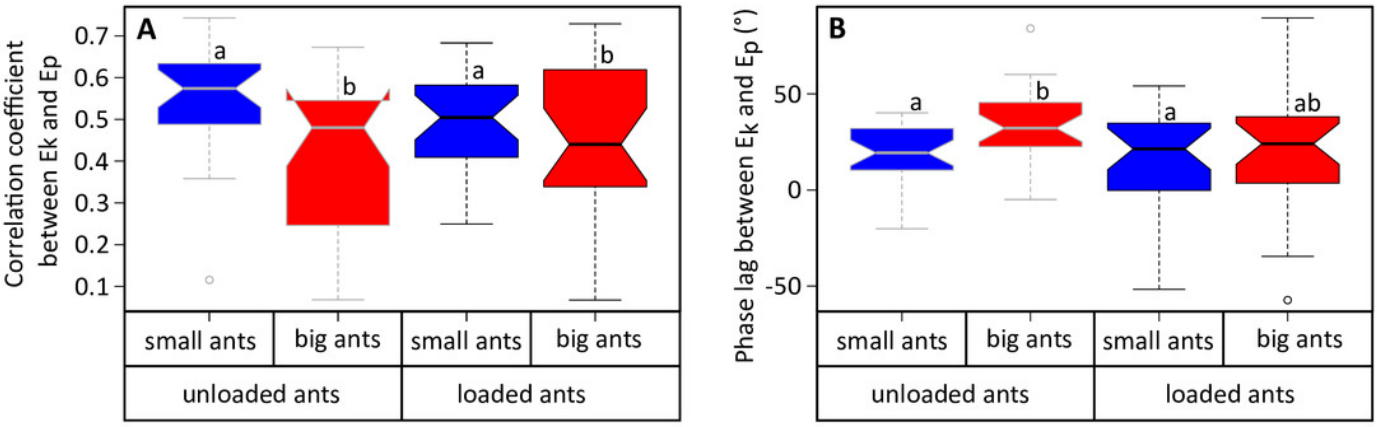

Figure 6

External mechanical work and power for unloaded ants.

A: external mechanical work ($F_{1,52}$ =1502, P<0.001) and **B**: external mechanical power ($F_{1,52}$ =717, P<0.001). The straight line gives the prediction of a linear regression model and the dashed lines the 95% confidence interval of the slope of the regression line (N= 54 ants).